Journal of Power Sources 195 (2010) 223–231

Contents lists available at ScienceDirect

Journal of Power Sources

journal homepage: www.elsevier.com/locate/jpowsour

Ion track grafting: A way of producing low-cost and highly proton conductive membranes for fuel cell applications

M.-C. Clochard[a,*], T. Berthelot[a], C. Baudin[a], N. Betz[a,1], E. Balanzat[b], G. Gébel[c], A. Morin[d]

[a] Laboratoire des Solide Irradiés, CEA - DSM/IRAMIS – CNRS UMR 7642 - Ecole Polytechnique, F-91128 Palaiseau, France
[b] CIMAP, CEA – CNRS – ENSICAEN BP 5133 F-14040 Caen, France
[c] CEA - DSM/INAC/SPrAM CEA-Grenoble 17 rue des Martyrs, F-38054 GRENOBLE Cedex 9, France
[d] CEA - DRT/LITEN/DTH/LCPEM CEA-Grenoble 17 rue des Martyrs, F-38054 GRENOBLE Cedex 9, France

ARTICLE INFO

Article history:
Received 17 March 2009
Received in revised form 22 May 2009
Accepted 9 July 2009
Available online 18 July 2009

Keywords:
Ion track grafting
Radiografting
Swift heavy ions
Proton conductivity
Polymer electrolyte membrane
Proton exchange membrane fuel cell

ABSTRACT

Proton conductive individual channels through a poly(vinyl di-fluoride) PVDF matrix have been designed using the ion track grafting technique. The styrene molecules were radiografted and further sulfonated leading to sulfonated polystyrene (PSSA) domains within PVDF. The grafting process all along the cylindrical ion tracks creates after functionalisation privileged paths perpendicular to the membrane plane for proton conduction from the anode to the cathode when used in fuel cells. Such ion track grafted PVDF-g-PSSA membranes have low gas permeation properties against H_2 and O_2. A degree of grafting (Y_w) of 140% was chosen to ensure a perfect coverage of PSSA onto PVDF-g-PSSA surface minimizing interfacial ohmic losses with the active layers of the Membrane Electrolyte Assembly (MEA). A three-day fuel cell test has been performed feeding the cell with pure H_2 and O_2, at the anode and cathode side respectively. Temperature has been progressively increased from 50 to 80 °C. Polarisation curves and Electrochemical Impedance Spectroscopy (EIS) at different current densities were used to evaluate the MEA performance. From these last measurements, it has been possible to determine the resistance of the MEA during the fuel cell tests and, thus the membrane conductivity. The proton conductivities of such membranes estimated during fuel cell tests range from 50 mS cm^{-1} to 80 mS cm^{-1} depending on the operating conditions. These values are close to that of perfluorosulfonated membrane such as Nafion® in similar conditions.

1. Introduction

One of the challenges of the twenty first century is to develop efficient low-cost membranes for fuel cell application, notably for the industrialisation of non-pollutant cars. The ideal membrane should satisfy to the following requirements: permeability lower than perfluorosulfonated membrane such as Nafion®, that is to say lower than 5 barrer at 80 °C when fully humidified, high proton conductivity 10^{-2} to 10^{-1} S cm^{-1} at high temperature and low water content, especially above 80 °C, a chemical stability in the fuel cell conditions, especially versus oxidation, reduction, hydrolysis, low dimensional changes upon swelling, a high mechanical stability and a sensitive price. Even the most used polymer electrolyte membranes in fuel cells applications, the Nafion® membranes from Dupont, do not completely fulfil these drastic requirements. Theses membranes consist of a hydrophobic fluorocarbon backbone assuring the mechanical support and hydrophilic sulfonic side chains for proton transfer. Despite some serious inconvenient such as a high cost (ca. US$ 850–800 m^{-2} for *Nafion*-117 sheet membranes [1]), a water swelling shortening the membrane life time and conductivity losses at high temperature, the Nafion® is still the reference today. Presently, only Gore Primea 5710 series membranes are really able to reach its fuel cell test performances and life time [2,3] but it is still a derivative of Nafion®.

Many other type of membranes have already been tested: (i) non-fluorinated membranes [4]: sulfonated copolymers of polystyrene-polybutadiene, polyethersulfone, polyphenylenesulfone [5,6], polyetherketone [4,7–9], polyarylene ethers [10], polyimides [11,12], polybenzimidazole [8,13–15], polyacrylates [16–18], oxadiazole-based polymers [19] and (ii) fluorinated membranes: trifluoroethylene (TFE) copolymers and many radiografted polystyrene or styrene derivatives onto fluorinated polymer such as ethylene tetrafluoethylene (ETFE) or PVDF [20–29]. Some of these new polymers are promising but the two main problems are a lower conductivity and stability in oxidizing conditions compared to Nafion® shortening the life time in fuel cell conditions [30–33].

* Corresponding author at: Laboratoire des Solides Irradiés, CEA/DSM/IRAMIS/LSI, Ecole Polytechnique, F-91128 Palaiseau, France. Tel.: +33 1 69 33 45 26; fax: +33 1 69 33 45 54.
E-mail address: marie-claude.clochard@polytechnique.edu (M.-C. Clochard).
[1] Deceaded.

0378-7753/$ – see front matter © 2009 Elsevier B.V. All rights reserved.
doi:10.1016/j.jpowsour.2009.07.016

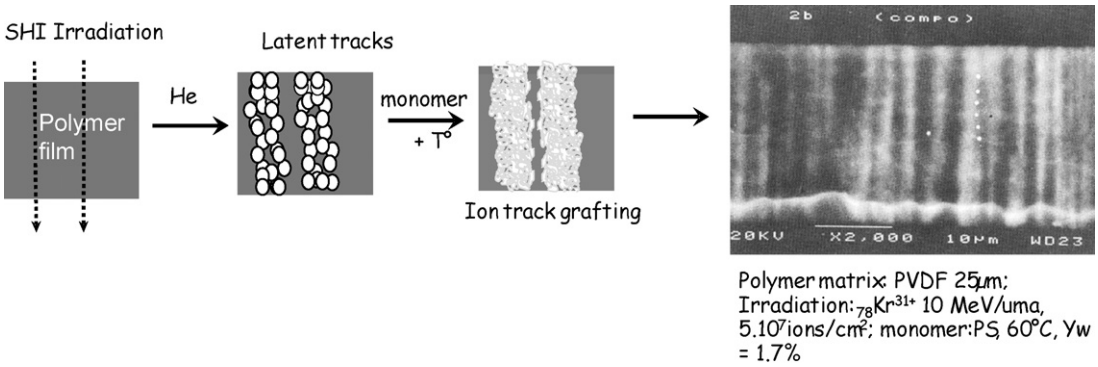

Fig. 1. Scheme of swift heavy irradiation of penetrating ions through a polymeric foil, the latent track formation and the subsequent ion grafting localised inside the latent track. Example: SEM micrograph of the cross-section of an ion-track grafted PVDF-g-PS membrane.

The lower proton conductivity can be compensated increasing the ion content but it is generally at the expense of the mechanical stability in water swollen conditions. Consequently, the trend is to reinforce theses new polymer electrolyte membranes either by adding some crosslinkers or by introducing an inorganic filler to improve the polymer membrane mechanical properties [34–40]. Radiation [41] to graft membranes is widely investigated because of the double effect: (i) functionalisation with proton conductive entities and (ii) creation of a three-dimensional network if the radiation dose is higher than the dose gel of the polymer or if a radiation sensitive crosslinker such as di-vinyl benzene is used during the formulation.

Until now, low ionising radiations such as electrons, γ-rays or X-rays ionising radiations have been used to radiograft homogeneously polymer foils [25,42,43]. The LSI in collaboration with the CIMAP uses a less studied kind of ionising radiation for polymer electrolyte membranes synthesis, swift heavy ions (SHI). Indeed, ions induce all along their trajectory through the solid a continuous trail of excitations and ionisations leading to the formation of a specific cylindrical damage called latent tracks. The final heterogeneous solid is then formed of latent tracks (or highly damaged cylindrical zones) and pristine areas. The latent tracks are radically active and allow the copolymerisation with vinyl monomers. Ion track grafting was first performed by Monnin and Blanford in 1973 [44] for detection of nuclear tracks. Since this pioneer work, a large majority of related publications has been written by N. Betz from the LSI [45–49]. Her unique experience in this field is still pursued today in our team.

The idea [50] was to ensure the mechanical and dimensional stability of the future proton exchange membrane stability by playing with SHI properties allowing to leave some pristine fluorinated polymer parts as a support matrix and to design proton conductive channels by radio-induced track grafting inside this same PVDF matrix (Fig. 1). This SHI processing is a unique way for creating nanocomposite membranes. PVDF is a very appropriate substrate because of its high chemical resistance, its good mechanical properties and its hydrophobic fluorocarbon backbone. The channels consist of high density of proton conductive entities interpenetrated with PVDF chains. All theses proton conductive entities are covalently bound to the PVDF support. The cost of such membranes was estimated by us from catalogue prices at no more than US$ 200 m^{-2} at a small production scale (ion-beam irradiation cost representing only 10% of the membrane price).

The present paper relies on fuel test performances of 40 μm thick PVDF-g-PSSA polymer electrolyte membranes obtained from SHI track grafting. EIS was used in parallel especially to determine the influence of the working parameters, such as outlet gas pressure, on the resistance of the MEA.

2. Experimental

2.1. Swift heavy ion radiation grafting: poly(PVDF-g-PS)

Prior to use, the 9 μm thick β PVDF films produced by Solvay (Belgium) were extracted in a Soxhlet apparatus with toluene, for 24 h. After drying at 60 °C under vacuum for 12 h, the samples were irradiated in an helium atmosphere at GANIL (Caen, France) with $_{78}Kr^{31+}$ at a specific energy of 10 MeV amu^{-1}. The electronic stopping power $(dE/dx)_e$ of the Kr ions was 40 MeV $cm^2.mg^{-1}$. The fluence (Φ) was 10^{10} ions cm^{-2}. For comparison purposes, other irradiation conditions were also used: gamma rays, and high energy oxygen and xenon beams. A SHI irradiation induces a heterogeneous dose distribution at the nanometric level. The doses quoted here correspond to the mean absorbed dose (D); D (Gy) = 1.6×10^{-7}. Φ (cm^{-2}). $(dE/dx)_e$ (MeV cm^2 mg^{-1}).

The irradiated films were grafted with pure styrene for 1 h at 60 °C according to a process previously reported [48]. The grafting yield is given by $Y_w = (W_f - W_i)/W_i$ (%) where W_f and W_i are the sample weights after and before grafting, respectively.

2.2. Functionalisation: poly(PVDF-g-PSSA)

After swelling during 20 min in dichloromethane (CH_2Cl_2) at room temperature, the grafted fluoropolymers, noted poly(PVDF-g-PS) were immersed in a 10 vol.% chlorosulfonic acid solution for 30 min in order to add sulfonic acid groups (SO_3H) on the phenyl ring of the polystyrene. The chlorosulfonation proceeded by two successive reactions: the first one total and the second reversible, leading to the formation of sulfonate (SO_3H) and chlorosulfonate (SO_2Cl) groups. A basic hydrolysis (NaOH 1 M, RT, 2 h) was then performed to act on the reversible reaction to convert the SO_2Cl groups in SO_3Na ones. Na^+ are exchanged by H^+ by immersion in 1 M H_2SO_4 during 3 h at room temperature in order to recover the sulfonic acid groups. PVDF-g-PSSA membranes were rinsed three times in deionised water and dried gently at 50 °C under vacuum for 12 h. The hydrolysis was followed using Energy Dispersive Spectrometer (EDS) coupled to Field Emission Scanning Electron Microscope (FESEM). The hydrolysis was considered to be complete when the Cl ions K-ray signal was completely suppressed. The functionalisation rate was around 60%.

2.3. Infrared spectroscopy measurements

FTIR spectra of the polymer films were carried out with a Nicolet Magna-IR™ 750 spectrometer equipped with a DTGS detector. Spectra were recorded in an Attenuated Total Reflection mode (ATR) using a diamond-crystal with single reflection. Experiments were carried out cumulating 32 scans at a resolution of 2 cm^{-1}.

2.4. High resolution magic angle spinning nuclear magnetic resonance (HR MAS NMR) spectroscopy

All experiments were performed with an Avance 500 spectrometer equipped with a triple resonance (^{1}H-^{13}C-^{31}P) HRMAS probe head. NMR rotors were standard ZrO_2 4 mm rotors without insert. Spinning speed corresponded to 5 kHz. Deuterated dimethylsulfoxide (dmso-d6) and dimethylformamide (dmf-d7) were purchased from Eurisotop (France). Each sample was prepared as follows: 80 μl of solvent was added to 8 mg of polymer and the mixture was heated at 100 °C for 1 h, so as to obtain a paste-like consistency. The resulting slurry was introduced into the HRMAS rotor using a simple pipette.

2.5. Ion exchange capacity

The ion exchange capacity (IEC) was measured following a conventional route. The membranes were first immersed in 1 M NaCl solution for 24 h at room temperature. The released protons were titrated against 0.01 M NaOH solution using phenolphthalein indicator. The IEC of the graft copolymer membranes was calculated using the following equation:

$$\text{IEC (mequiv. g}^{-1}) = \frac{V \cdot N_{OH}}{m}$$

where V is the volume of NaOH at the equivalence, N_{OH} is the normality of NaOH and m the total weight of polymer. The reported IEC values were the mean of five measurements and the average estimated error was ±8%.

2.6. Water uptake

Water uptake was determined by weighing the vacuum-dried membrane and the fully equilibrated membrane with water. The membrane sample was wiped with an adsorbent paper to remove excess water and the sample was weighted. The water uptake was determined as follows:

$$\text{Water uptake (wt\%)} = \frac{m_f - m_i}{m_i} \times 100$$

where m_f and m_i are the weights of wet and dried membranes respectively. The reported water uptake values were the mean of at least 3 measurements and the average estimated error was ±10%.

2.7. Proton conductivity

The membrane in-plane proton conductivity was determined by impedance spectroscopy using a Materials Mates 7260 impedancemeter and a home-made conductivity cell. A series of 1 mm thick gold lines inserted in a flat polymer support are used as electrodes and spaced from 0.2 cm to 1.75 cm. Pieces of membranes (1 cm × 2 cm) equilibrated at least 2 h in liquid water are placed between the two flat supports. The conductivity was measured with different combinations of electrodes in order to average measured values and to avoid any effect of local heterogeneities. The reported values were the mean of at least 4 measurements and the average estimated error was ±5%. The frequency was carried from 5 MHz to 100 Hz.

2.8. MEA preparation

Before starting the fuel cell test, the ion track grafted PVDF-g-PSSA membrane was fully hydrated by immersion in ultrapure water for 2 h. The membrane was then directly piled up into a 5 cm^2 single cell designed by Quintech between two commercial gas diffusion electrodes E-LAT LT 140EW-SI from BASF. These electrodes were made with 30 wt% Pt/C and the catalyst loading of each was 0.5 mg cm^{-2}. The stress on the membrane has been calculated taking into account the compressive behaviours of the electrode and the gasket and is about 1 MPa.

2.9. Fuel cell test

Fuel cell tests have been performed in co-flow configuration using a home-made fuel cell test bench feeding the cell with pure H_2 and O_2 at the anode and cathode sides, respectively. The relative humidity of each gas was controlled thanks to a bubbler and modified by the temperature of and by regulation of the temperature of the water. Relative humidity was calculated as the ratio of the theoretical partial pressures of water at the temperature of the bubbler and at the cell temperature.

Constant gas flows were used (40 ml min^{-1} for both hydrogen and oxygen up to 800 mA cm^{-2}). Therefore, the gas stoichiometries depend on the current density below this value and correspond to about 1.5 and 3 at 800 mA cm^{-2} for H_2 and O_2 respectively. Above 800 mA cm^{-2} hydrogen gas flow was increased to keep a constant stoichiometry of 1.5.

The cell temperature was controlled and progressively increased from 50 °C to 80 °C. During the test, the temperature of the bubblers was kept constant around 30 °C whatever the cell temperature inducing a decrease of the relative humidity as the cell temperature increased. A 2 absolute bars pressure was applied except for a specific experiment performed at 80 °C, 4 absolute bars and 100% relative humidity for each gas. Polarisation curves were recorded with a linear scan rate. The cell was operated continuously during 50 h.

2.10. In situ EIS measurements

Electrochemical Impedance Spectroscopy measurements have been performed in galvanodynamic mode with a Biologic potentiostat/impedancemeter VMP2 with a 20 A booster. The complex impedance was measured between 10 kHz and 0.3 Hz in each experimental condition at different current densities. For each frequency decade, 10 measurements were made and the amplitude was at a maximum at 10% of the value of the current. For each frequency, the values were recorded after waiting 4 periods and were average on 4 periods.

3. Results and discussion

3.1. Ion track grafted PVDF-g-PSSA membranes

Ion track grafting technique allows the creation of channels of grafted polyelectrolyte all along the linear ion tracks inside a thin PVDF film (Fig. 1). Structuring the matter is very interesting for generating privileged paths for proton conduction without inducing any further porosity. Consequently, such membranes have low gas permeation properties against H_2 and O_2. Similar PVDF-g-PSSA membranes have already been synthesized and characterized in our group for mainly biomedical purposes by FTIR [51,52], XPS [47,53], X-ray scattering and scanning electron studies [43,54]. The grafting heterogeneity of fluoropolymers irradiated by swift heavy ions in comparison to γ-ray was then well defined. In the present study, a high grafting yield of Y_w = 140% was chosen in order to radiograft not only inside the latent tracks but also to cover completely the membrane surface [43] in order to have the maximum interfacial exchange with the active layer of the PEMFC. At this grafting level, the initial 9 μm thick PVDF in beta phase reach 40 μm of total thickness. The translucent initial PVDF aspect turns to a white shiny colour in the grafted PS part (Fig. 2).

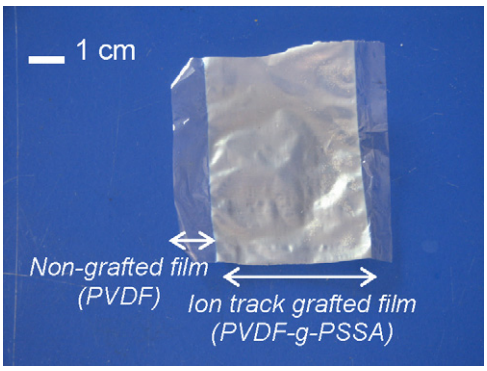

Fig. 2. Photograph of an ion track grafted PVDF-g-PSSA membrane (fluence 10^{10} cm^{-2}): white part corresponds to the radiografted part (grafting yield of 140 wt%), translucent part corresponds to the non-irradiated part (SHI beam width = 4 cm).

The FTIR spectra of the PVDF-g-PS and PVDF-g-PSSA obtained are in good agreement with that obtained previously [52] (Fig. 3). It was found under FTIR total reflexion mode a 100% covering of PS with the disappearance of PVDF CH_2 stretching vibration bands at

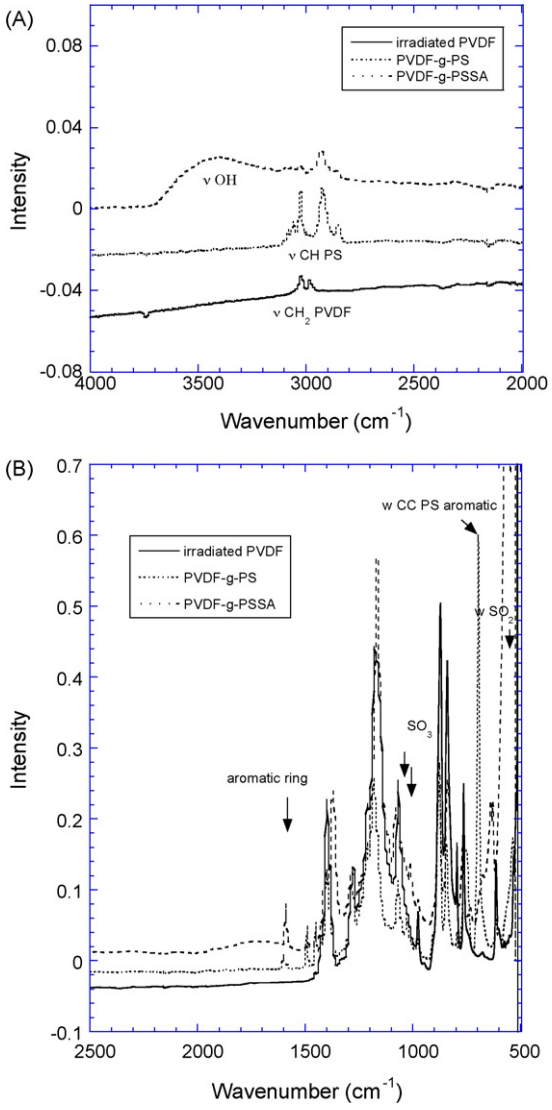

Fig. 3. FTIR spectra of the $^{78}Kr^{31+}$ irradiated PVDF, ion grafted PVDF with polystyrene (PVDF-g-PS) – Y_w = 140% – and subsequent sulfonation (PVDF-g-PSSA): (A) 4000–2000 cm^{-1}, region (B) 2500–500 cm^{-1} region.

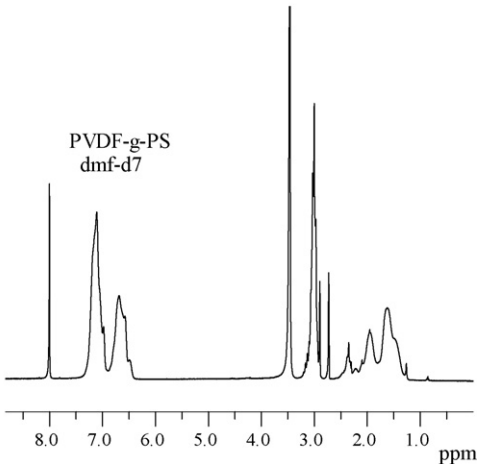

Fig. 4. HRMAS ^{1}H spectrum of ion track grafted PVDF-g-PS membrane (fluence 10^{10} cm^{-2}) swollen in deuteriated DMF.

2985 cm^{-1} and 3025 cm^{-1} in favour to the typical PS bands in that region.

To complete PVDF-g-PSSA membrane characterisation, in volume and time, we have used liquid NMR spectroscopy. After irradiation, some radicals on PVDF films may recombine together to form covalent bonds leading to cross-linked films. As a matter of fact, films are not soluble in DMF. Attempts to obtain solution spectra by classical liquid NMR probe were not satisfactory. Solid state spectra, in such a case, generally display poor resolution. A solution to this dilemma is to swell the films with the DMF and to acquire spectra while spinning at magic angle. Figs. 4 and 5 display the obtained ^{1}H spectra for ion track grafted PVDF-g-PS and PVDF-g-PSSA membranes respectively. In Fig. 4, ^{1}H spectrum displays 2 large peaks at 6.6 ppm and 7.1 ppm corresponding to the aromatic groups of PS. Two other peaks at 1.6 ppm and 2 ppm are attributed to CH_2 and CH of PS respectively. The triplet at 3 ppm corresponds to the PVDF. Peak integrations allow us to determine a grafting yield of 140 wt% in agreement with the gravimetric value. The PVDF-g-PS was well-swollen in DMF. After sulfonation, the solubility has changed and the swelling was no longer efficient in DMF. DMSO was found more appropriate. The need to change the solvent to acquire HRMAS NMR spectra shows a change in the hydrophilic property of the initial hydrophobic PVDF-g-PS membrane. Fig. 5 illustrates the ^{1}H spectrum of PDVF-g-PSSA in DMSO. A typical acidic proton peak appears at 13.1 ppm while the aromatic groups in the zone ranging from 6 ppm to 8 ppm seems to be less resolved and the CH and CH_2 of PSSA collapsed as it was previously described for PSSA in liq-

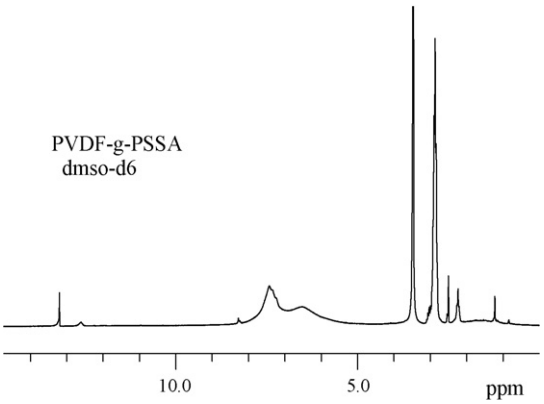

Fig. 5. HRMAS ^{1}H spectrum of ion track grafted PVDF-g-PSSA membrane (fluence 10^{10} cm^{-2}) swollen in deuteriated DMSO.

Table 1
IEC, water uptake and proton conductivities of ion track grafted PVDF-g-PSSA with 140 wt% PS content at various gas relative humidities, gas supplies and temperatures.

Polymer electrolyte membrane	IEC (mequiv. g^{-1})	Water uptake (wt%) at room temperature	λ ($[H_2O]/[SO_3H]$)	RH (%)	Gas feed rate (Bar)	T (°C)	σ (mS cm^{-1})
Ion track grafted PVDF-g-PSSA	2.97	17	3.7	35	2	50	36
				20	2	60	51
				15	2	70	55
				100	2	80	60
				100	4	80	61
Nafion®	0.95	40[a]	22[a]	100	4	80	80

[a] From literature [25,28,60].

uid ^{1}H NMR [55]. Unfortunately, in the latter case, the quantitative approach was not possible.

IEC values are indicative of the actual ion exchange sites available for proton conductivity. The higher values of IEC are then desirable to achieve higher proton conductivity in polymer electrolyte membranes. Ion track grafted PVDF-g-PSSA membrane with a Y_w of 140% exhibited a IEC of 2.97 mequiv. g^{-1}, which is three times higher than that of Nafion®117 (Table 1). The water uptake of ion track grafted PVDF-g-PSSA is also presented in Table 1. The water uptake was found to be two times inferior to that of the value of Nafion®117. From literature [25], the water uptake for PVDF-g-PSSA copolymer membrane obtained from homogeneous e-beam irradiation is higher than Nafion®117; for example, a IEC of 1 in such a membrane corresponds to a water uptake of 52%. It means that our membrane structuration is very effective in constraining the water uptake inside the local hydrophilic channels. The high stiffness of the hydrophobic PVDF polymer matrix limits the swelling of the membrane to less than 20% in one direction only (membrane thickness).

3.2. Proton conductivities

Fig. 6 displays the proton conductivities of PVDF-g-PSSA membranes radiografted from different irradiation sources as a function of the grafting yield. Gamma irradiation provides a homogeneous irradiation through the solid. The induced radicals are consequently homogeneously distributed in the polymer bulk. The grafting occurs from the surface to the inner part of the PVDF film. It is then necessary to reach a threshold value of the grafting yield to connect each grafting fronts and to obtain percolation. For this reason the proton conductivities have been measured at low grafting yields. A series of SHI radiografted sulfonated membranes irradiated with Xe and O ions (fluence 7×10^9 ions cm^{-2} deposited dose 0.5 kGy and 10^9 ions cm^{-2} deposited dose 38 kGy respectively)

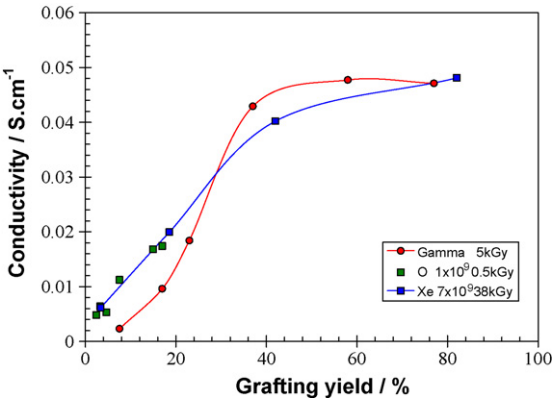

Fig. 6. Proton conductivities versus grafting yields for radiografted PVDF-g-PSSA membranes in latent tracks using two different type of ions, O and Xe and radiografted PVDFg-PSSA membranes using gamma irradiation.

were prepared and compared to Gamma irradiated (deposited dose 5 kGy). For the two types of SHI membranes with different ions, fluences and deposited doses the results are very similar indicating that these parameters are not first order parameters. Since in-plane conductivities are measured one could have expected a lower conductivities for SHI membranes compared to gamma irradiated materials. Since the conductivity is measured with electrodes located on each membrane side the limiting process is thus the through plane conductivity. A grafting yield of 10 wt% in 25 μm thick β-PVDF membrane corresponds to this threshold. For ion track grafted PVDF-g-PSSA membranes, proton conductivities were recorded even at very low grafting yields – below 10 wt% – because the grafting diffusion is favoured through the PVDF film all along the tracks. As a matter of fact, for SHI, the conductivity only depends on Y_w and not on D or $(dE/dx)_e$. Besides, at least, when Y_w is smaller than 30%, the conductivity obtained by SHI is higher than with gamma rays. This indicates that the cylindrical nanocomposite structure enhances the proton conductivity. The benefit of the specific structure induced with SHI is not restricted to the improvement of the mechanical and dimensional stability but also concerns proton conductivity. It is worth noting that the proton conductivities measured *ex situ* for large grafting yields (e.g. Fluence = 10^{10} tracks cm^{-2}; Y = 140 wt%; $\sigma = 120 \pm 6$ mS cm^{-1}) are closer to the value determined *in situ* by EIS in the fuel cell experiments.

3.3. Fuel cell performances

The conditioning of such new membranes was just a simple membrane immersion in acidic water. The test was started at rather low temperature (around 30 °C) in order to avoid membrane dehydration and to check for the absence of H_2 crossover. The pressure was progressively increased up to 2 absolute bars with a flow of 40 ml min^{-1} of fully humidified pure H_2 and O_2. The stabilised open circuit voltage (OCV) was quite low (860 mV) but no evidence of membrane leakage has been observed. The current was slowly increased up to 40 mA cm^{-2} and the voltage was around 610 mV. The cell temperature was then increased up to 50 °C (35% RH) and after 45 min, a polarisation curve was recorded (Fig. 7). At that stage, low performances were obtained (OCV 835 mV and 6.5 mA cm^{-2} at 700 mV). Three hypotheses are drawn to explain the low current density: poor quality of the membrane-electrode interface, a partial dehydration of the membrane or of the ionomer within the active layer. Indeed, because of the chemical composition of the membrane and the scale of proton conducting channel structures which covers about 74% of the surface, the interface between the membrane and the commercial electrode which contains perfluorosulfonic acid (PFSA) ionomer could be worst than with Nafion®. So, impedance spectroscopy measurements have been performed in order to better understand the imitating phenomena (Fig. 8).

Whatever the current density, the first semi-circle intercepts the abscise axis for a frequency of approximately 2 kHz when the imaginary part of the impedance is equal to zero revealing a pure ohmic

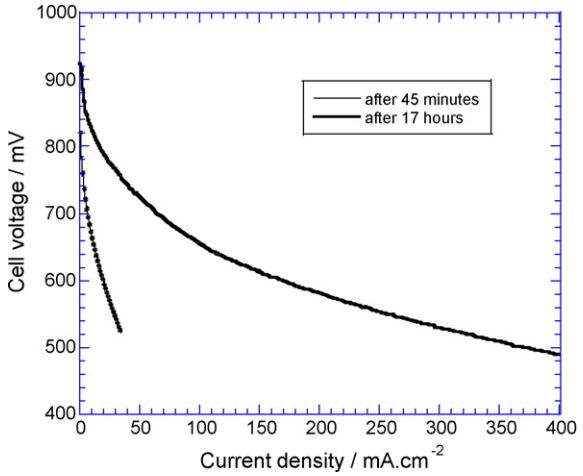

Fig. 7. Polarisation curves recorded during the conditioning step, after 45 min. and 17 h of operation at 50 °C with pure H_2 and O_2 at 2 bars and 35%RH.

behaviour. The corresponding specific resistance corresponds to the sum of all the ohmic phenomena, meaning ionic resistance of the membrane, electronic resistance of the electrodes and of the single cell test fixture components, interface resistance between all the electronic conducting cell components. Assuming that the

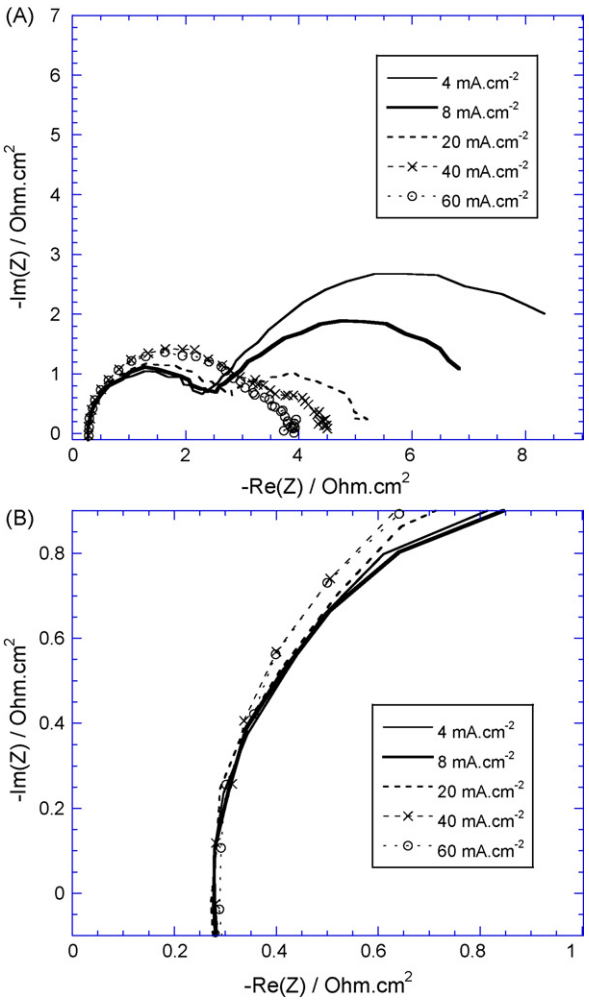

Fig. 8. Impedance spectroscopy measurements recorded during the conditioning step, after 45 min of operation at 50 °C with pure H_2 and O_2 at 2 bars and 35%RH (A. full recording; B. zoom of higher frequencies region).

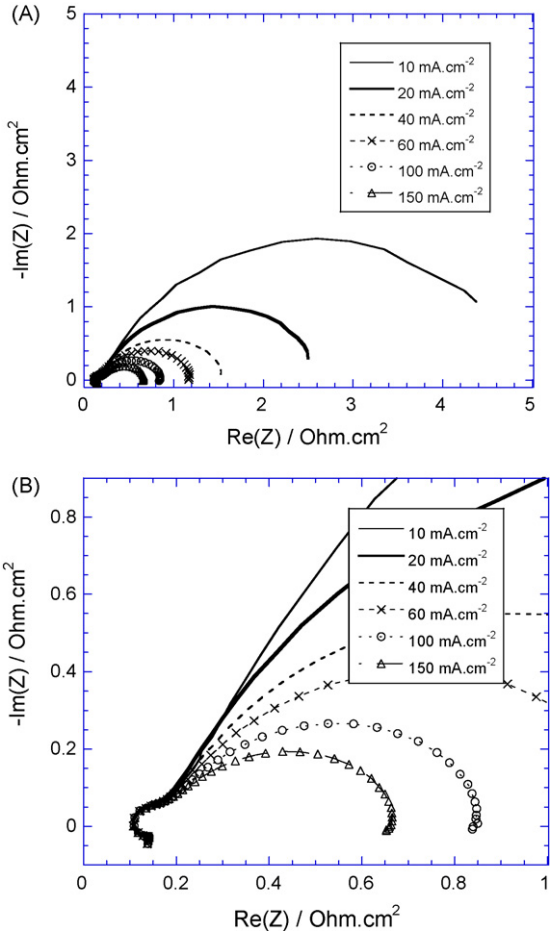

Fig. 9. Impedance spectroscopy measurements recorded during the conditioning step after 17 h of operation at 50 °C with pure H_2 and O_2 at 2 bars and 35%RH (A. full recording; B. zoom of higher frequencies region).

electronic resistance of the cables, the single cell test fixture components and the interfaces between them are negligible compared to the resistances within the MEA (components and interfaces: R_{MEA}), it appears clearly that R_{MEA} does not depend on the current density and is about 56 mOhm or 280 mOhm cm^2 (Fig. 9). With 10 mOhm cm^2 [56] as electronic resistance for each electrode (R_{elec}) and about 5 mOhm cm^2 [57] as contact resistance between the electrodes and the monopolar plates ($R_{contact}$), the ionic resistance of the membrane and membrane/electrodes interfaces is about 250 mOhm cm^2. Assuming negligible interface ohmic losses, 5 cm^2 as active area and an homogeneous distribution of water content on the whole surface area and within the membrane thickness, a membrane conductivity of about 1.6×10^{-2} S cm^{-1} can be estimated. This is a quite high value with regard to the cell performance and to the low water uptake when expressed as the number of water molecules per sulfonic acid group ($\lambda \approx 3$). For the same water content, the proton conductivity of Nafion® is more or less similar, i.e. 2×10^{-2} S cm^{-1} at 80 °C [58]. This could probably be explained by the structure of these membranes with proton conducting channels through the whole thickness of the membrane. The discrepancy between the fairly high proton conductivity and the very low fuel cell performance can be understood considering the contributions of all the overpotentials through the analysis of the low frequency resistance in the EIS spectra. This total specific resistance (R_T) corresponds to the sum of the ohmic resistance (R_{MEA}) and the polarisation resistance (R_{Pol}): $R_T = R_{MEA} + R_{Pol}$. For example, at 20 mA cm^{-2} the impedance value is 1 Ohm, that is to say that the specific resistance is about 5000 mOhm cm^2, which is

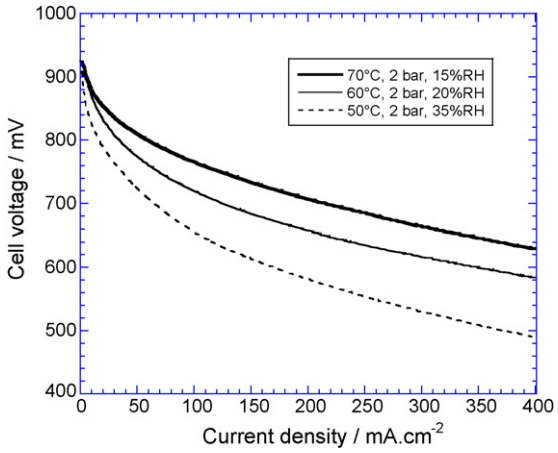

Fig. 10. Comparison of polarisation curves recorded at 50 °C, 60 °C and 70 °C with pure H_2 and O_2 at 2 bars.

in very good agreement with the one calculated from the slope of the polarisation curve.

In the Niquist plot, two main contributions are observed (Fig. 8). The first contribution with a characteristic frequency of about 200 Hz increases with the current density. It may be due either to a poor membrane-electrode interface or to the drying of the anode caused by the electroosmosis of water from the anode to the cathode and/or by a lack of water back-flow from the cathode to the anode side. Since the low current densities do not favour electroosmosis, the first hypothesis has thus to be considered. The second contribution with a characteristic frequency of a few Hz decreases as the current density increases. It is likely due to the activation overpotential of the oxygen reduction reaction (ORR) since the signal in this frequency range is characteristic of the charge transfer phenomena at the cathode side. It is a high value (about 1000 mOhm cm^2 at 60 mA cm^{-2}) probably because the low current density does not favour an efficient cathode hydration. The low performances at the beginning of the test are mainly due to charge transfer overpotentials on both the cathode and anode side originating from either a drying of the anode or a poor membrane-electrode interface which does not give an ohmic contribution at high frequency.

After 17 h of operation (50 °C, 2 absolute bars and 35% RH), the cell performances considerably increased and the OCV reached about 920 mV. A second polarisation curve was recorded (Fig. 7). While the cell voltage usually reaches the equilibrium in approximately 8 h with Nafion® in the same operating conditions and electrodes, the equilibrium is still not reached with SHI grafted membranes. A possible explanation of this delayed increase of performance is that the improvement of the membrane electrodes interfaces requires a sufficient MEA hydration especially at the anode and slowly favours a better water management. This is observed on impedance spectra by the disappearance of the contribution at 200 Hz. Only the contribution of the charge transfer at the cathode side which decreases as the current density increases remains (Fig. 9). The MEA specific resistance (110 mOhm cm^2) leads to a membrane proton conductivity of 5×10^{-2} S cm^{-1} (Fig. 9).

The performance progressively increased with the temperature up to 70 °C (Fig. 10) and the specific resistance decreases (110, 80 and 75 mOhm cm^2 at 50 °C, 60 °C and 70 °C respectively (Fig. 11). It worth noting that the cell temperature increase from 50 °C to 70 °C induces a decrease of the gas inlet relative humidity from 35% to 15% RH which should not favour the membrane hydration and consequently, an increase of both the membrane conductivity (8×10^{-2} S cm^{-1} and 9×10^{-2} S cm^{-1} at 60 °C and 70 °C, respectively) and the cell performance. Complementary experiments will

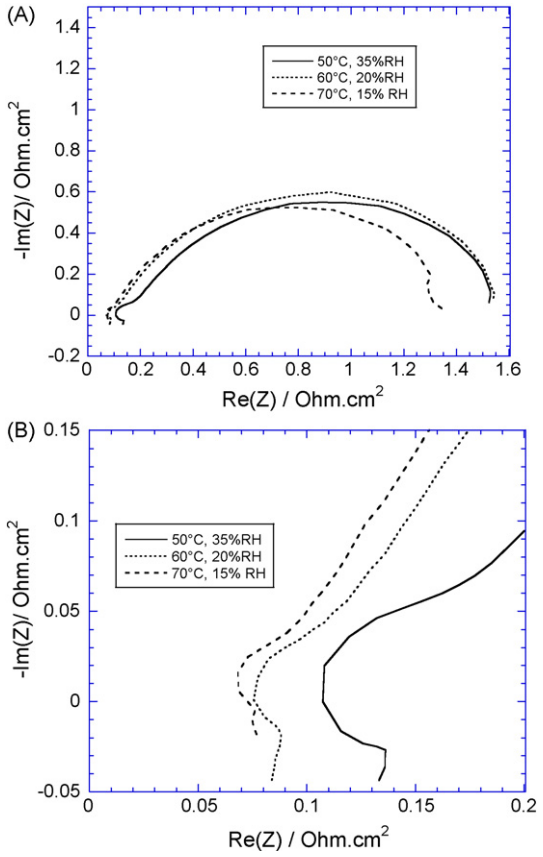

Fig. 11. Impedance spectroscopy measurements recorded at 40 mA cm^{-2} and 50 °C, 60 °C and 70 °C with pure H_2 and O_2 at 2 bars (A. full recording; B. zoom of higher frequencies region).

be necessary to complete our understanding on the origin of the fuel cell performance (membrane and electrode hydration, electroosmosis, water back-diffusion, membrane reorganization, . . .).

Both the OCV and the fuel cell performance increase with increasing cell temperature (OCV is respectively 920, 970, 1006 mV at 70 °C, 80 °C, 100% RH, 2 and 4 bars) (Fig. 12). There is no significant change in MEA specific resistance between 2 and 4 bars at 80 °C 100% RH but the ORR charge transfer resistance decreases as the pressure increases (Fig. 13) as expected for a higher reactant concentration on the electrodes. The conclusions extracted from EIS spectra of the polarisation curves are in good agreement. In addi-

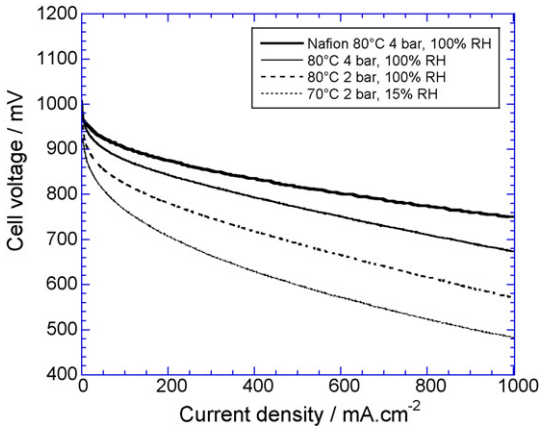

Fig. 12. Comparison of polarisation curves recorded at 80 °C with pure H_2 and O_2 and 100%RH at 2 and 4 bars.

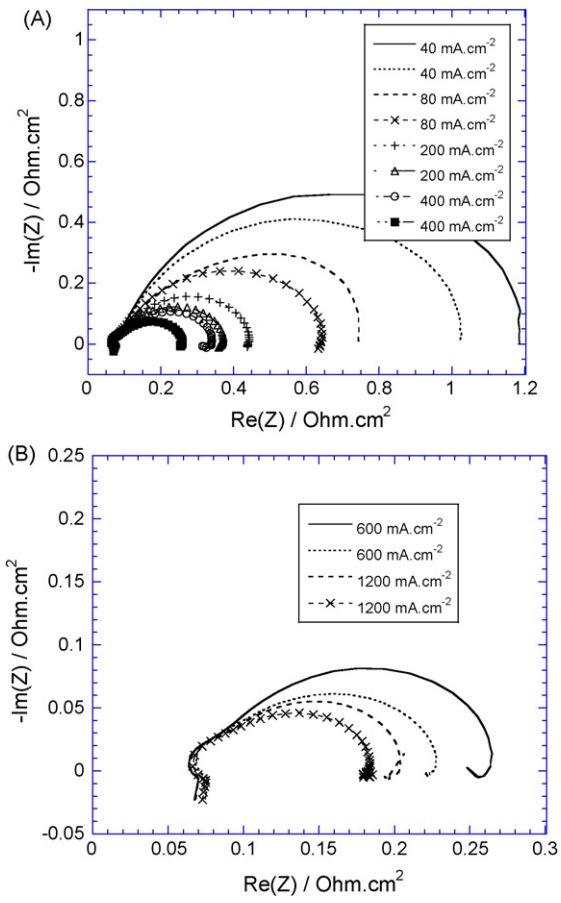

Fig. 13. Comparison of the impedance spectra recorded at 80 °C with pure fully humidified H_2 and O_2 at 2 bars (full symbol) and 4 bars (open symbols) (A. from 40 mA cm^{-2} to 400 mA cm^{-2}; B. from 600 mA cm^{-2} to 1200 mA cm^{-2}).

tion, the last point of the IES spectra at low frequencies related to polarisation curve is similar to the one of the left end side at high frequency. It means that the resistance of the membrane stays constant. At 80 °C, 4 bars with pure and fully humidified H_2 and O_2, the cell voltage is 670 mV at 1 A cm^{-2}. The performance is only a little lower than with a Nafion® NRE212 membrane (50 μm) with hot-pressed commercial electrodes which is a very encouraging result (Fig. 12).

4. Conclusion

PVDF-g-PSSA membrane obtained after SHI irradiation have been synthesized, characterized and tested in fuel cell continuously during 50 h in different operating conditions using pure H_2 and O_2. Despite poor performance during the starting procedure at low temperature, performance at 80 °C and 100% RH are finally similar to those obtained with Nafion® 212 membranes (50 μm). In these operating conditions, the proton conductivity calculated from the MEA specific resistance is the same as for Nafion®, e.g. 8×10^{-2} S cm^{-1}. This could be due to the unique structure of this membrane which have straight and large (~50 nm) proton conducting channels with high ion exchange capacity. The increase in performance at the beginning of the test and the behaviour of the MEA in the different operating conditions could be due to improvement of either interfaces and/or the water back-flow within the membrane. Work is in progress in order to understand more clearly the behaviour of the membrane since we obtain very promising results with these first tests. Notably, it will be interesting to study the mechanical support of the matrix before and after fuel cell test and compare the behaviour with other kind of PVDF-g-PSSA structures.

Indeed these membranes appear as very interesting materials since many parameters can now be optimized acting on the radiation and grafting conditions, the proton exchange functionalities (for example replacing the sulfonic acid (–SO_3H) groups by phosphonic acid (–PO_3H_2) groups known to be more efficient at high temperature) or on the grafted segment nature to increase both the stability and the acidity. Consequently, more chemistry is ongoing to test multi-functionalisations all along the proton conductive channels [59].

Acknowledgement

This work was supported by CEA-DRT/LITEN (Grenoble, France) in the framework of NTE French program.

References

[1] R.P.W.J. Struis, M. Quintilii, S. Stucki, J. Membr. Sci. 177 (2000) 215–223.
[2] S. Kim, M.M. Mench, J. Power Sources 174 (2007) 206–220.
[3] W. Liu, M. Crum, ElectroChem. Soc. Trans. 3 (2006) 531–540.
[4] B. Smitha, S. Sridhar, A.A. Khan, J. Membr. Sci. 259 (2005) 10–26.
[5] V. Saarinen, K.D. Kreuer, M. Schuster, R. Merkle, J. Maier, Solid State Ionics 178 (2007) 533–537.
[6] G. Maier, J. Meier-Haack, In Fuel Cells II; Springer-Verlag Berlin, Berlin, 216 (2008) pp. 1–62.
[7] X. Zhu, Y. Liang, H. Pan, X. Jian, Y. Zhang, J. Membr. Sci. 312 (2008) 59–65.
[8] D.J. Jones, J. Rozière, J. Membr. Sci. 185 (2001) 41–58.
[9] V. Ramani, S. Swier, M.T. Shaw, R.A. Weiss, H.R. Kunz, J.M. Fenton, J. Electrochem. Soc. 155 (2008) B532–B537.
[10] D.H. Choi, J. Lee, O. Kwon, J.Y. Kim, K. Kim, J. Power Sources 178 (2008) 677–682.
[11] C.H. Lee, C.H. Park, Y.M. Lee, J. Membr. Sci. 313 (2008) 199–206.
[12] C. Marestin, G. Gebel, O. Diat, R. Mercier, Fuel Cells Ii, vol. 216, Springer-Verlag Berlin, Berlin, 2008, pp. 185–258.
[13] J.S. Wainright, J.T. Wang, D. Weng, R.F. Savinell, J. Electrochem. Soc. 142 (1995) 121–123.
[14] J. Jouanneau, R. Mercier, L. Gonon, G. Gebel, Macromolecules 40 (2007) 983–990.
[15] J. Peron, E. Ruiz, D.J. Jones, J. Rozière, J. Membr. Sci. 314 (2008) 247–256.
[16] Y. Shen, J. Xi, X. Qiu, W. Zhu, Electrochim. Acta 52 (2007) 6956–6961.
[17] J.K. Choi, D.K. Lee, Y.W. Kim, B.R. Min, J.H. Kim, J. Polym. Sci. Part B - Polym. Phys. 46 (2008) 691–701.
[18] B.H. Liu, Z.P. Li, L.L. Chen, J. Power Sources 108 (2008) 530–534.
[19] D. Gomes, J. Roeder, M.L. Ponce, S.P. Nunes, J. Power Sources 175 (2008) 49–59.
[20] H.P. Brack, M. Wyler, G. Peter, G.G. Scherer, J. Membr. Sci. 214 (2003) 1–19.
[21] H.S. Huang, C.Y. Chen, S.C. Lo, C.J. Lin, S.J. Chen, L.J. Lin, Appl. Surf. Sci. 253 (2006) 2685–2689.
[22] J. Qiu, L. Zhao, M. Zhai, J. Ni, H. Zhou, J. Peng, J. Li, G. Wei, J. Power Sources 177 (2008) 617–623.
[23] Y.W. Kim, D.O. Lee, K.J. Lee, J.H. Kim, Eur. Polym. J. 44 (2008) 932–939.
[24] V. Saarinen, O. Himanen, T. Kallio, G. Sundholm, K. Kontturi, J. Power Sources 163 (2007) 768–776.
[25] S.D. Flint, R.C.T. Slade, Solid State Ionics 97 (1997) 299–307.
[26] T. Lehtinen, G. Sundholm, S. Holmberg, F. Sundholm, P. Björnbom, M. Bursell, Electrochem. Acta 43 (1998) 1881–1890.
[27] R. Souzy, B. Ameduri, B. Boutevin, G. Gébel, P. Capron, Solid State Ionics 176 (2005) 2839–2848.
[28] Y.W. Kim, J.K. Choi, J.T. Park, J.H. Kim, J. Membr. Sci. 313 (2008) 315–322.
[29] H.P. Brack, D. Ruegg, H. Buhrer, M. Slaski, S. Alkan, G.G. Scherer, J. Polym. Sci. Part B-Polym. Phys. 42 (2004) 2612–2624.
[30] B. Mattson, H. Ericson, L.M. Torell, F. Sundholm, Electrochim. Acta 45 (2000) 1405–1408.
[31] S. Kundu, K. Karan, M. Fowler, L.C. Simon, B. Peppley, E. Halliop, J. Power Sources 179 (2008) 693–699.
[32] M. Prasanna, E.A. Cho, T.-H. Lim, I.-H. Oh, Electrochem. Acta 53 (2008) 5434–5441.
[33] V.O. Mittal, H.R. Kunz, J. Fenton, J. Electrochem. Soc. 153 (2006) A1755–A1759.
[34] A. Anis, A.K. Banthia, S. Bandyopadhyay, J. Power Sources 179 (2008) 69–80.
[35] R. Souzy, B. Ameduri, Progr. Polym. Sci. 30 (2005) 644–687.
[36] H.G. Herz, K.D. Kreuer, J. Maier, G. Scharfenberger, M.F.H. Schuster, W.H. Meyer, Electrochim. Acta 48 (2003) 2165–2171.
[37] Y. Zhang, H. Zhang, C. Bi, X. Zhu, Electrochim. Acta 53 (2008) 4096–4103.
[38] P. Bebin, M. Caravanier, H. Galiano, J. Membr. Sci. 278 (2006) 35–42.
[39] K. Valle, P. Belleville, F. Pereira, C. Sanchez, Nat. Mater. 5 (2006) 107–111.
[40] A. Mokrini, M.A. Huneault, P. Gerard, J. Membr. Sci. 283 (2006) 74–83.
[41] S.A. Gursel, L. Gubler, B. Gupta, G.G. Scherer. Fuel Cells I, vol. 215, Springer-Verlag Berlin, Berlin, 2008, pp. 157–217.
[42] S. Hietala, E.M. Skou, F. Sundholm, Polymer 40 (1999) 5567–5573.

[43] C. Aymes-Chodur, N. Betz, M.-C. Porte-Durrieu, C. Baquey, A. Le Moël, Nucl. Instrum. Meth. Phys. Res. B 177 (1999) 377–385.
[44] M.M. Monnin, G.E. Blanford, Science 181 (1973) 743–744.
[45] N. Betz, C. Ducouret, A. Le Moël, Nucl. Instrum. Meth. Phys. Res. B 91 (1994) 151–156.
[46] N. Betz, Nucl. Instrum. Meth. Phys. Res. B 105 (1995) 55–62.
[47] N. Betz, S. Dapoz, M.-J. Guittet, Nucl. Instrum. Meth. Phys. Res. B 131 (1997) 252–259.
[48] N. Betz, A. Le Moël, J.-P. Duraud, E. Balanzat, C. Darnez, Macromolecules 25 (1992) 213–219.
[49] N. Betz, E. Balanzat, A. Le Moël, J.-P. Duraud, Radiation Effects Defects Solids 126 (1993) 221–224.
[50] M.-C. Clochard, T. Berthelot, CEA, France, 2007, p. FR0757875.
[51] C. Ducouret, E. Petersohn, N. Betz, A. Le Moël, Spectrochim. Acta 51A (1995) 567–572.
[52] S. Dapoz, N. Betz, A. Le Moël, J. Chim. Phys. 93 (1996) 58–63.
[53] S. Dapoz, N. Betz, M.-J. Guittet, A. Le Moël, Nucl. Instrum. Meth. Phys. Res. B 105 (1995) 120–125.
[54] G. Gébel, E. Ottomani, J.-J. Allegraud, N. Betz, A. Le Moël, Nucl. Instrum. Meth. Phys. Res. B 105 (1995) 145–149.
[55] C.M. Fernyhough, R.N. Young, A.J. Ryan, L.R. Hutchings, Polymer 47 (2006) 3455–3463.
[56] S. Escribano, J.F. Blachot, J. Etheve, A. Morin, R. Mosdale, J. Power Sources 156 (2006) 8–13.
[57] I. Nitta, T. Hottinen, O. Himanen, M. Mikkola, J. Power Sources 171 (2007) 26–36.
[58] Y. Sone, P. Ekdunge, D. Simonsson, J. Electrochem. Soc. 143 (1996) 1254–1259.
[59] T. Berthelot, M.-C. Clochard, CEA, France, 2007, p. FR0757873.
[60] T.E. Springer, T.A. Zawodzinski, S. Gottesfeld, J. Electrochem. Soc. 138 (1991) 2334–2342.